Virologica Sinica 37 (2022) 731–739

Contents lists available at ScienceDirect

Virologica Sinica

journal homepage: www.keaipublishing.com/en/journals/virologica-sinica
www.virosin.org

Research Article

# LNP-CpG ODN-adjuvanted varicella-zoster virus glycoprotein E induced comparable levels of immunity with Shingrix™ in VZV-primed mice

Ning Luan [1], Han Cao [1], Yunfei Wang, Kangyang Lin, Cunbao Liu [*]

*Institute of Medical Biology, Chinese Academy of Medical Sciences and Peking Union Medical College, Kunming 650118, China*

ARTICLE INFO

*Keywords:*
Varicella zoster virus (VZV)
Subunit vaccine
Adjuvant
Lipid nanoparticle (LNP)
CpG oligodeoxynucleotide (CpG ODN)
AS01B
Humoral immunity
Cell-mediated immunity (CMI)

ABSTRACT

Latent varicella-zoster virus (VZV) may be reactivated to cause herpes zoster, which affects one in three people during their lifetime. The currently available subunit vaccine Shingrix™ is superior to the attenuated vaccine Zostavax® in terms of both safety and efficacy, but the supply of its key adjuvant component QS21 is limited. With ionizable lipid nanoparticles (LNPs) that were recently approved by the FDA for COVID-19 mRNA vaccines as carriers, and oligodeoxynucleotides containing CpG motifs (CpG ODNs) approved by the FDA for a subunit hepatitis B vaccine as immunostimulators, we developed a LNP vaccine encapsulating VZV-glycoprotein E (gE) and CpG ODN, and compared its immunogenicity with Shingrix™ in C57BL/6J mice. The results showed that the LNP vaccine induced comparable levels of gE-specific IgG antibodies to Shingrix™ as determined by enzyme-linked immunosorbent assay (ELISA). Most importantly, the LNP vaccine induced comparable levels of cell-mediated immunity (CMI) that plays decisive roles in the efficacy of zoster vaccines to Shingrix™ in a VZV-primed mouse model that was adopted for preclinical studies of Shingrix™. Number of IL-2 and IFN-γ secreting splenocytes and proportion of T helper 1 (Th1) cytokine-expressing $CD4^+$ T cells in LNP-CpG-adjuvanted VZV-gE vaccinated mice were similar to that of Shingrix™ boosted mice. All of the components in this LNP vaccine can be artificially and economically synthesized in large quantities, indicating the potential of LNP-CpG-adjuvanted VZV-gE as a more cost-effective zoster vaccine.

## 1. Introduction

Varicella-zoster virus (VZV, also known as human herpesvirus 3) is a neurotropic and lymphotropic virus with double-stranded DNA, and most children come in contact VZV before 10 years of age (Lee et al., 2021; Ogunjimi et al., 2009). As its name indicates, VZV causes two distinct diseases, i.e., varicella/chickenpox, upon primary infection, and zoster/shingles, when latent viruses in the sensory ganglia are reactivated. One or two doses of approximately 1000–10,000 plaque-forming units (PFU) of live attenuated VZV (e.g., the Oka strain developed by Takahashi in 1974 and approved by the FDA in 1995) could offer 90% efficacy against varicella (Baxter et al., 2013; Takahashi et al., 1974). Unfortunately, the Oka strain could also stay dormant in the sensory ganglia and be reactivated as wild strains do, which may cause zoster with similar chances when the immune system is senescent (e.g., aging) or compromised (e.g., during infection by HIV or clinical immunosuppressive treatment) (Arruti et al., 2017; Breuer, 2018; Hales et al., 2013; Krause and Klinman, 2000; Leung et al., 2011; Levin et al., 2017). Zoster affects one in three people during their lifetime, with approximately 15% of serious cases of postherpetic neuralgia (PHN) showing that the pain persists for at least 3 months and cannot be effectively alleviated by antiviral medications (Gershon et al., 2015; Johnson and Rice, 2014).

Unlike varicella vaccines, which depend on humoral immunity to prevent VZV infection, cell-mediated immunity (CMI) plays decisive roles in the efficacy of zoster vaccines (Asada, 2019; Gilbert et al., 2014; Haberthur et al., 2011; Steain et al., 2014; Weinberg and Levin, 2010). Zoster vaccines play a therapeutic role in the control or elimination of reactivated VZV in infected cells. Due to its ability to boost preexisting CMI that was induced by primary wild-type VZV exposure or varicella vaccination, a single subcutaneous dose of an attenuated virus as high as 19,400 PFU was approved by the FDA in 2005 as a zoster vaccine (Zostavax® from Merck & Co., Inc., Kenilworth, NJ, USA). Unfortunately, there are two disadvantages for this live attenuated zoster vaccine. In addition to the difficulties in manufacturing and maintaining the

* Corresponding author.
*E-mail address:* cunbao_liu@163.com (C. Liu).
[1] Ning Luan and Han Cao contributed equally to this work.

https://doi.org/10.1016/j.virs.2022.06.002
Received 2 March 2022; Accepted 1 June 2022
Available online 6 June 2022

necessary high titers of this live-attenuated virus, the protective rate decreases from 70% for people 50–59 years of age to less than 38% for people older than 70 years (Gilderman et al., 2008; Oxman et al., 2005).

As one of the most abundant VZV glycoproteins, glycoprotein E (gE) is essential for viral replication and transmission between ganglionic cells (Berarducci et al., 2006; Malavige et al., 2008; Mo et al., 2000, 2002; Moffat et al., 2004). The conserved and potential neutralization epitopes and T cell epitopes of gE make it an ideal target as a subunit vaccine antigen (Garcia-Valcarcel et al., 1997; Zhu et al., 2016). With the inclusion of the AS01B adjuvant system to enhance CMI targeting the extracellular domain of gE, two intramuscular doses of the subunit zoster vaccine Shingrix™ (developed by GlaxoSmithKline (GSK), Rockville, MD, USA, and approved by the FDA in 2017) showed protective rates of 96.6%, 97.4% and 91.3% for people aged 50–59, 60–69 and older than 70 years, respectively (Chlibek et al., 2013; Cohen, 2015; Cunningham et al., 2016, 2018; Haumont et al., 1996; Leroux-Roels et al., 2012). One of the key components of AS01B (i.e., QS21) for inducing CMI is a polysaccharide mixture extracted from the bark of *Quillaja saponaria*, which is distributed in the temperate regions of South America (Upadhyay et al., 2018; Wang, 2021). Whereas, limited supply, infeasible synthesis and strict quality control during the extraction processes of QS21 have made Shingrix™ very expensive (approximately 150–200 USD per dose, and two doses are needed).

In our previous reports, we showed that encapsulation of an economical oligodeoxynucleotide containing CpG motifs (CpG ODN) into poly(lactic-co-glycolic acid) (PLGA)-based nanoparticles was beneficial in therapeutic vaccine targeting TC-1-xenografted tumor through induction of antigen-specific CMI responses (Liu et al., 2018a, 2018b). This adjuvant system also showed potential roles in inducing VZV-gE CMI responses (Wang et al., 2021). While CpG ODN has been FDA-approved as immunostimulants for hepatitis B subunit vaccine, the use of PLGA vectors has been FDA-approved for chemical medicines only, not vaccines. In addition, through the double-emulsion (w/o/w) solvent evaporation method, the efficiency of encapsulation of CpG ODN by PLGA is less than 30%, which needs to be improved (Iqbal et al., 2015; Wang et al., 2021).

In a recent study, we showed that ionizable lipid nanoparticles (LNPs) that were recently approved by the FDA as carriers for severe acute respiratory syndrome coronavirus 2 (SARS-CoV-2) mRNA vaccines could efficiently encapsulate VZV-gE and CpG ODN (Cao et al., 2021a). This subunit vaccine induced both potential VZV neutralization and CMI responses, but it was not tested in a VZV-primed mouse model that was adopted for preclinical studies of Shingrix™, and no positive controls were used (Cao et al., 2021a; Dendouga et al., 2012). In this study, with Shingrix™ as a positive control, we showed that LNP-CpG-adjuvanted VZV-gE induced humoral immunity and CMI response comparable to those induced by Shingrix™ in a VZV-primed mouse model, showing promise as a safe and economical zoster vaccine candidate.

## 2. Materials and methods

### 2.1. Vaccine preparation

CHO cell-expressed VZV gE extracellular domain protein (supplied by AtaGenix Laboratory Co., Ltd., Wuhan, China) was diluted to 5 μg/mouse/dose in 25 μL of phosphate-buffered saline (PBS, pH 7.4) and mixed with the same volume of aluminum hydroxide (Thermo Fisher, Eugene, OR, USA) for alum-adjuvanted vaccines.

LNP vaccines were prepared using a modified procedure described in our previous report (Cao et al., 2021a). Briefly, lipids (from AVT Pharmaceutical Technology Co., Ltd., Shanghai, China) were dissolved in ethanol in the following molar ratio: ionizable lipid:1, 2-distearoyl-sn-glycero-3-phosphocholine (DSPC):cholesterol: 1,2-dimyristoyl-rac-glycero-3-methoxypolyethylene glycol-2000 (DMG-PEG2000) = 50:10:38.5:1.5. Protein gE and phosphodiester CpG ODN (weight ratio of CpG ODN BW006:CpG ODN 2395 = 1:1) were dissolved with 100 mmol/L citrate buffer (pH 4.0), mixed thoroughly, and combined with the lipid mixture at a ratio of 3:1 with a microfluidic mixer (Precision Nanosystems, Vancouver, BC, Canada). The formulations were dialyzed against PBS, concentrated with a centrifugal filtration tube (Millipore), passed through a 0.22-μm syringe filter (PALL), and stored at 4 °C until use.

The diameter and polydispersity index (PDI) of the particles were tested with a Zetasizer Nano ZS particle size analyzer (Malvern Panalytical, Malvern, UK). After lysis by 0.1 mol/L NaOH containing 0.1% SDS (m/v) overnight, the concentration of the loaded gE protein was detected by the bicinchoninic acid protein assay (Beyotime, Shanghai, China), and the encapsulation efficiency was calculated as follows: encapsulation efficiency = the amount of loaded gE/the initial amount of gE input in citrate buffer × 100%. The loaded nucleic acids were detected with the Quant-iT OliGreen ssDNA Reagent Kit (Thermo Fisher, Eugene, OR, USA).

### 2.2. Mouse studies

Specific-pathogen-free (SPF) female C57BL/6J mice (6–8 weeks, 20–22 g) were supplied by the Central Animal Service of the Institute of Medical Biology, Chinese Academy of Medical Sciences (IMB, CAMS), randomly divided into 7 groups with 6 mice in each group and maintained in SPF conditions before use. The PBS control group was subcutaneously (SC) injected with 100 μL PBS in the scruff of the neck, followed by intramuscularly (IM) injection with two doses of 50 μL PBS in the tibialis muscle at 4-week intervals. The Prime control group was SC injected with 4000 PFU Oka strain (Changchun BCHT Biotechnology Co., Ltd., Changchun, China) suspended with 100 μL PBS to mimic natural infection (Dendouga et al., 2012), followed by IM injection with two doses of 50 μL PBS at 4-week intervals. With a 1/10 human dose of Shingrix™ (produced by GSK biological SA, Wavre, Belgium) as a positive control, the 3 primed groups (including primed alum, primed LNP-CpG and primed Shingrix™) were SC injected with 4000 PFU Oka strain at the dose of 100 μL, followed by IM injection with two doses of 50 μL immunogens at 4-week intervals. The 2 unprimed groups (including LNP-CpG and Shingrix) were IM injected with 50 μL immunogen twice as other groups without prime. Two weeks after the last immunization, whole blood samples and spleen cells were collected as described elsewhere (Cao et al., 2021b). After centrifugation at 1000 ×*g* for 30 min, serum samples were obtained and stored at −80 °C before use.

### 2.3. gE protein-specific antibodies detection by enzyme-linked immunosorbent assay (ELISA)

The levels of gE protein-specific antibodies in serum samples collected from immunized mice were determined by ELISA. VZV gE dissolved in PBS was used to precoat 96-well microplates at a final concentration of 2 μg/mL. After incubation overnight at 4 °C, the plates were washed with PBST (0.05% (v/v) polysorbate 20 in PBS) 3 times. Five percent (w/v) skim milk in PBS was used to block the plates for one hour, and the plates were incubated with twofold-diluted mouse sera (diluted from 2000 to 4,096,000) for another 1 h. Goat anti-mouse IgG conjugated with horseradish peroxidase (HRP) (1:10,000. Bio-Rad, Hercules, CA, USA) was used as the detection antibody. After addition of the mixed substrate 3,3,5,5-tetramethylbenzidine (TMB, BD, CA, USA) for 5 min, 1 mol/L sulfuric acid was added to stop the reaction. The absorbance at 450 nm was determined with a spectrophotometer (BioTek Instruments, Inc., Winooski, VT, USA). IgG titers were defined by the end-point dilutions with a cutoff signal intensity of OD450 = 0.15, and IgG titers that show OD450 lower than 0.15 at a dilution of 1:2000 were defined as 100 for calculations (Liu et al., 2021).

### 2.4. Cytokine analysis

Spleen cells were suspended in Roswell Park Memorial Institute (RPMI, Thermo Fisher) 1640 medium supplemented with 10% (v/v)

fetal bovine serum (FBS, Biological Industries, Cromwell, CT, USA) and penicillin-streptomycin (Thermo Fisher) at a final concentration of $1 \times 10^7$ cells/mL. Then, 100 μL of splenocytes was added to each well of a 96-well plate (Corning Inc., Corning, NY, USA). The protein gE dissolved in PBS was added to each well to a final concentration of 10 μg/mL, and the same volume of 12-myristate 13-acetate (PMA) + ionomycin (DAKEWE, China) was used as a positive control. After incubation for 24 h at 37 °C in a 5% $CO_2$ atmosphere, the supernatant of the cells was collected, and the levels of IL-2 and IFN-γ were determined by ELISA. Briefly, unconjugated IL-2 (3 μg/mL) and IFN-γ (4 μg/mL) antibodies (Invitrogen, USA) dissolved in PBS were used to coat the 96-well plates for 16 h at 4 °C. After blocking with 5% (w/v) skim milk at 37 °C for another 1 h, 50 μL of cell supernatant was added to each well, and the plates were incubated for 3 h at room temperature. PBS-dissolved standard mouse IL-2 and IFN-γ proteins (Peprotech, USA) were used to generate a standard curve. Biotin-conjugated antibodies against IL-2 and IFN-γ (2 μg/mL, Invitrogen, USA) and HRP-conjugated streptavidin (1 μg/mL, Biolegend, USA) were subsequently incubated for 1 h and 30 min, respectively. The reaction was terminated and examined as described above in the antibody detection section.

### 2.5. ELISPOT assay

Splenocytes ($3 \times 10^5$ cells/well) of immunized mice were seeded in 96-well plates for further analysis with enzyme-linked immunospot (ELISPOT) assay kits (BD, San Diego, CA, USA, catalog number 551076 for IL-2 and 551,083 for IFN-γ) according to the manufacturer's protocol. The protein gE at a final concentration of 20 μg/mL was used to stimulate gE-specific T cell responses, and the same volume of PMA + ionomycin was used as a positive control. Spots were counted with an ELISPOT reader system (Autoimmun Diagnostika GmbH, Strassberg, Germany) (Wang et al., 2021).

### 2.6. Flow cytometry

All the reagents below were purchased from Biolegend (San Diego, CA, USA). A total of $1 \times 10^6$ splenocytes were incubated with 10 μg/mL protein gE at 37 °C with 5% $CO_2$ for 2 h, and 5 μg/mL brefeldin A was then added. Then the mixture was incubated overnight under the same conditions to block cytokine release. After washing with staining buffer, 100 μL of Zombie NIR™ was added to each vial, and the vials were incubated for 30 min. Then, 5 μg/mL anti-CD16/CD32 antibodies were added, and the splenocytes were incubated at 4 °C for 10 min to block nonspecific binding of Fc receptors. Thereafter, PC5.5 anti-mouse CD4, BV510 anti-mouse CD44, and BV421 anti-mouse CD62L antibodies were added, and the samples were incubated at 4 °C for another 30 min. After washing with permeabilization buffer, PE-tagged anti-mouse IFN-γ and APC-tagged anti-mouse IL-2 antibodies were added, and the samples were incubated in the dark at room temperature for 30 min. After staining, the cells were gated (forward and side scatter, FSC/SSC), and samples with more than 20,000 $CD4^+$ T cells were analyzed with a CytoFLEX flow cytometer (Beckman, Indianapolis, IN, USA) and FlowJo V10 software (BD, Franklin Lakes, NJ, USA).

### 2.7. Statistical analysis

The data were analyzed by GraphPad Prism 9.2 (GraphPad Software Inc., La Jolla, CA, USA) and are expressed as the mean ± standard deviation (SD). Significant differences among experimental groups were analyzed by ordinary one-way analysis of variance (ANOVA) followed by Tukey's multiple comparisons test, comparing the mean of each group with the mean of every other group. Asterisks represent the $P$ value classification: $^*P < 0.05$; $^{**}P < 0.01$; $^{***}P < 0.001$; $^{****}P < 0.0001$.

## 3. Results

### 3.1. LNPs efficiently encapsulated gE and CpG ODN with uniformed particle size

LNP vaccines were prepared using a modified procedure described in our previous report (Cao et al., 2021a) and diagrammed as Fig. 1A. A total of 7.5 μg gE was included in each dose of LNP vaccine according to our previous experience (Cao et al., 2021a). The average encapsulation efficiency of the gE protein was 60.7% (Fig. 1B), which resulted in 4.55 μg of gE in each dose of prepared LNP on average, approximately equal to the amounts of the alum-adjuvanted vaccines or 1/10 single-dose Shringrix™ (5 μg). In addition, 15 μg of CpG ODN was added to each dose of the LNP vaccine. The mean value of the CpG ODN encapsulation efficiency was 72.54% (Fig. 1C), which resulted in 10.88 μg of CpG ODN in each dose of prepared LNP on average. The LNP was averagely 162.73 nm in diameter (lowest diameter 160.6 nm, largest diameter 164.3 nm, Fig. 1D), and showed good uniformity with polydispersity index (PDI, a measure of the heterogeneity of a sample based on size) of the particles as low as 0.218 on average (Fig. 1E).

### 3.2. LNP-encapsulated gE and CpG ODN induced potent humoral immune responses

Mice immunization scheme was shown in Fig. 2A. Forty-two C57BL/6J mice were randomly divided into 7 groups with 6 mice in each group. The PBS control group was SC injected with 100 μL PBS, and then boosted by IM injection with PBS at 4-week intervals twice. The prime control and primed groups were SC injected with 4000 PFU Oka strain. Then prime control group was boosted by IM injection with two doses of 50 μL PBS at 4-week intervals while the three primed groups (including primed alum, primed LNP-CpG and primed Shingrix™) were IM injected with two doses of immunogens at 4-week intervals. The 2 unprimed groups (including LNP-CpG and Shingrix) were IM injected with 50 μL immunogens twice without prime. Two weeks after the last immunization, gE-specific IgG titers were analyzed by ELISA (Fig. 2B).

Mice in the prime control group showed no gE-specific IgG antibodies, similar to mice in the PBS control group (Fig. 2B). Primed mice group boosted with Shingrix™ showed an average IgG titer of 117,333, which was 1.76 times higher than that of the primed mice boosted with the LNP vaccine (mean IgG titer of 66,667, $P = 0.0481$) and 7.65 times higher than that of the primed mice boosted with alum adjuvants (mean IgG titer of 15,333). Interestingly, unprimed mice immunized with either Shingrix™ or the LNP vaccine showed slightly higher gE-specific IgG titers (mean IgG titer of 149,333, $P = 0.4419$ for Shingrix™ immunized mice and mean IgG titer of 117,333, $P = 0.0481$ for the LNP vaccine immunized mice) than the corresponding Oka strain primed mice.

### 3.3. LNP encapsulated gE and CpG ODN induced cytokine responses at levels comparable to that boosted with Shingrix™

T cell responses induced by vaccination were evaluated two weeks after the last immunization, and splenocytes from each mouse were collected for cytokine analysis (Fig. 3A and B). As determined by ELISA, the average IL-2 level was 1143 pg/mL in the supernatant of splenocytes from primed mice immunized with Shingrix™ after gE stimulation, which was significantly higher than that in the primed mice immunized with the LNP vaccine (mean level of 779 pg/mL, $P = 0.0235$) (Fig. 3A). Unprimed mice immunized with either Shingrix™ or the LNP vaccine showed relatively low IL-2 levels (mean level of 668 pg/mL for Shingrix™, $P = 0.0014$ and mean level of 486.1 pg/mL for the LNP vaccine, $P = 0.113$) than that in the corresponding primed mice. The IFN-γ levels were comparable between the Shingrix™ and LNP vaccine-immunized mice, regardless of whether they were primed (mean level of 3662 pg/mL for Shingrix™ and mean level of 3908 pg/mL for the LNP vaccine, $P = 0.983$) or not (mean level of 1510 pg/mL for Shingrix™ and mean level

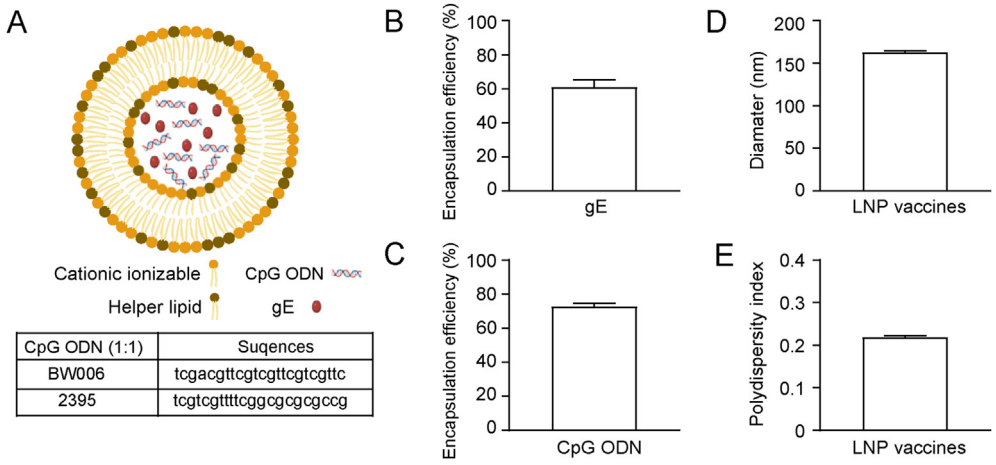


| CpG ODN (1:1) | Suqences |
|---|---|
| BW006 | tcgacgttcgtcgttcgtcgttc |
| 2395 | tcgtcgttttcggcgcgcgccg |

**Fig. 1.** Characterization of lipid nanoparticle (LNP) vaccines. **A** Diagram of LNP vaccines. Encapsulation efficiency of varicella-zoster virus glycoprotein E (gE) (**B**) and oligodeoxynucleotide containing CpG motifs (CpG ODN) (**C**). **D** The average diameter of LNP vaccine. **E** LNP vaccine polydispersity index (PDI) showing particle uniformity. Tests were repeated three times, and the data are shown as the mean ± SD (standard deviation).

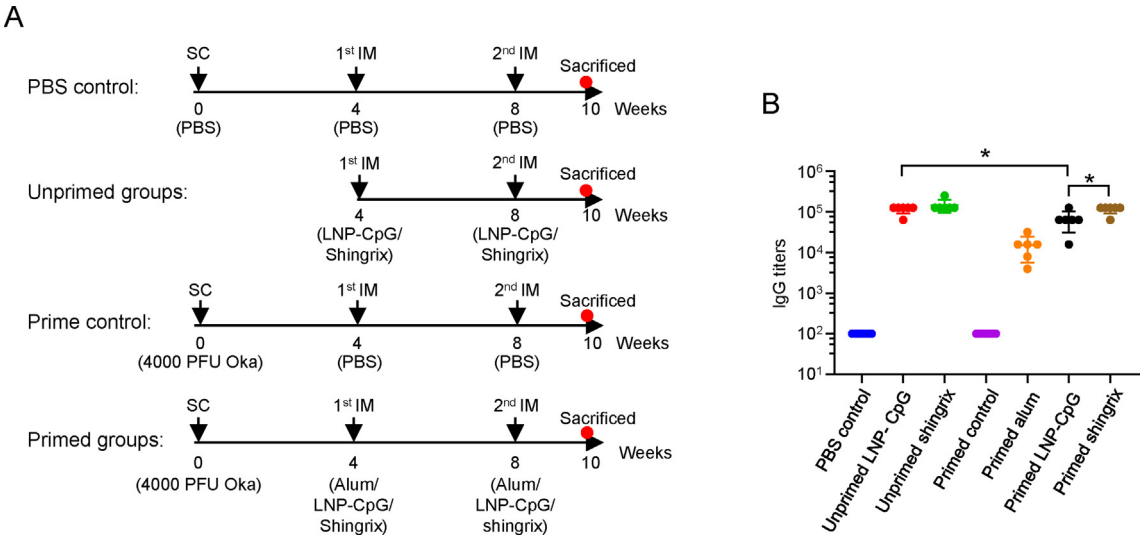


**Fig. 2.** Immunization schedule and gE-specific IgG titers. **A** Immunization schedules for different mice groups. Mice were randomly divided into 7 groups (N = 6) and immunized with PBS or Oka strain with 4000 PFU, then boosted two times with four weeks interval. Mice were sacrificed two weeks after the last immunization and serum or splenocytes were collected for analysis. **B** gE-specific IgG titers induced by different immune strategies were detected by ELISA. Points represent individual mice. The data were compared using one-way analysis of variance (ANOVA) followed by Tukey's multiple comparisons test, comparing the mean of each group with the mean of every other group. *, $P < 0.05$.

of 1513 pg/mL for the LNP vaccine, $P > 0.9999$), and primed mice showed higher IFN-γ levels than unprimed mice ($P < 0.0001$) for both Shingrix™ and the LNP vaccines (Fig. 3B).

Regarding ELISPOT analysis, the number of IL-2-secreting cells after gE stimulation was comparable between the Shingrix™ and the LNP vaccine-immunized mice, regardless of whether they were primed (mean number of 181 per $3 \times 10^5$ splenocytes for Shingrix™ and mean number of 204 per $3 \times 10^5$ splenocytes for the LNP vaccine, $P = 0.8273$) or not (mean number of 117.3 per $3 \times 10^5$ splenocytes for Shingrix™ and mean number of 124.2 per $3 \times 10^5$ splenocytes for the LNP vaccine, $P = 0.9996$) (Fig. 3C and D). The number of IFN-γ-secreting cells after gE stimulation was also comparable between Shingrix™ and LNP vaccine-immunized mice, regardless of whether they were primed (mean number of 276.3 per $3 \times 10^5$ splenocytes for Shingrix™ and mean number of 200.5 per $3 \times 10^5$ splenocytes for the LNP vaccine, $P = 0.1612$) or not (mean number of 157.8 per $3 \times 10^5$ splenocytes for Shingrix™ and mean number of 159.3 per $3 \times 10^5$ splenocytes for the LNP vaccine, $P > 0.9999$) (Fig. 3E and F). Besides, primed mice showed higher spots numbers than unprimed mice for both Shingrix™ and the LNP immunized groups.

### 3.4. *LNP-encapsulated gE and CpG ODN induced T helper 1 (Th1) cytokine-expressing CD4$^+$ T cells at levels comparable to that boosted with Shingrix™*

To further verify the phenotypes of responding T cells, splenocytes from each mouse were collected for flow cytometry analysis two weeks after the last immunization (Fig. 4A). The proportion of IL-2-expressing CD4$^+$ T cells after gE stimulation was comparable between Shingrix™ and LNP vaccine-immunized mice, regardless of whether they were primed (mean value of 0.2375% for Shingrix™ and mean value of 0.1880% for the LNP vaccine, $P = 0.8913$) or not (mean value of 0.2147% for Shingrix™ and mean value of 0.1555% for the LNP vaccine, $P = 0.985$) (Fig. 4B). The proportion of IFN-γ secreting cells after gE stimulation was also comparable between the Shingrix™ and the LNP vaccine-immunized mice, regardless of whether they were primed (mean

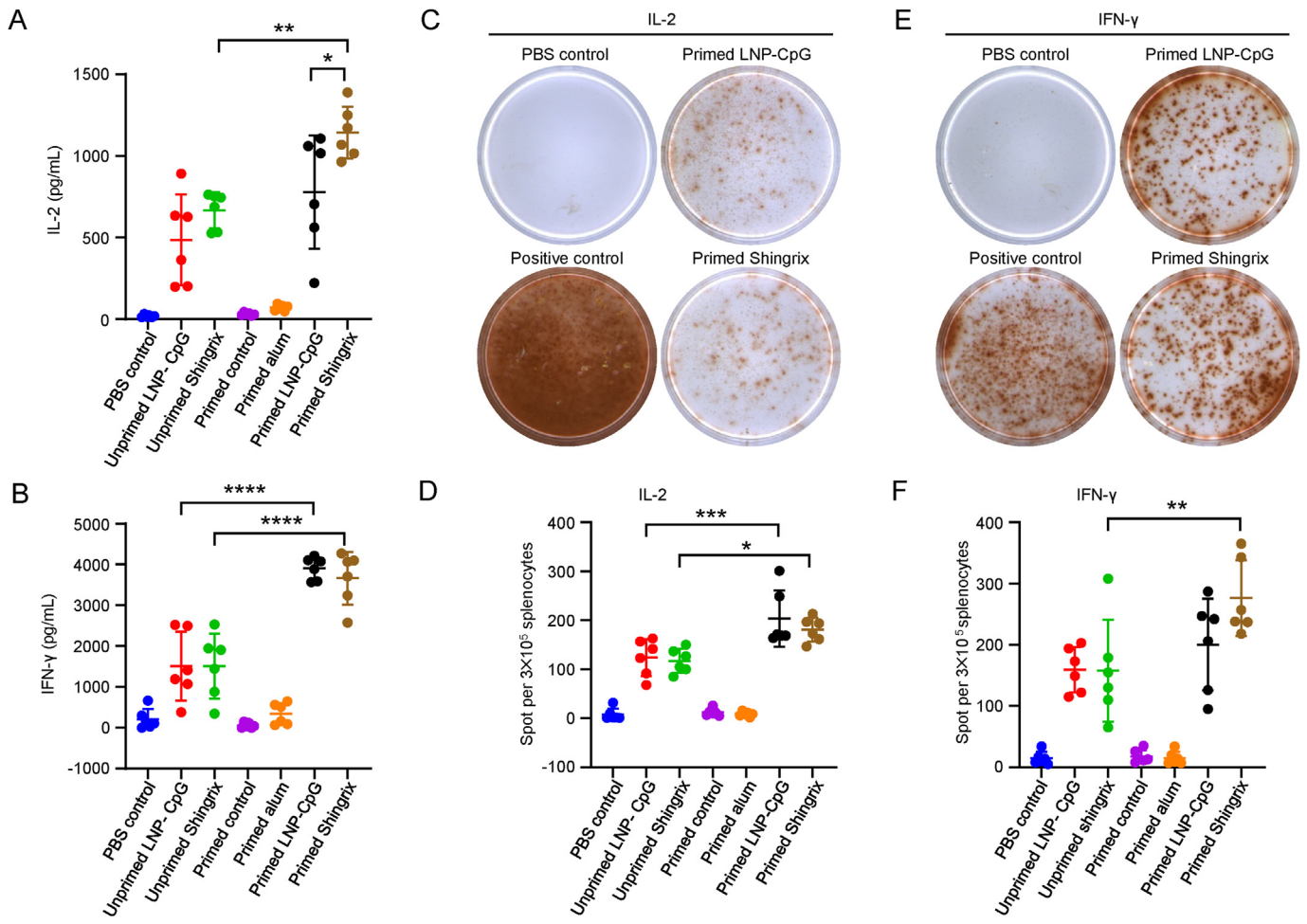


**Fig. 3.** LNP vaccines induced cytokine responses at levels comparable to Shingrix™ in immunized mice. IL-2 (**A**) and IFN-γ (**B**) secreted by splenocytes upon stimulation with 10 μg/mL gE were detected by ELISA. **C** Representative images of IL-2-producing splenocytes in the enzyme linked immunospot (ELISPOT) assay, and numbers of IL-2-producing splenocytes (**D**) were calculated from the ELISPOT assay after 20 μg/mL gE stimulation. **E** Representative images of IFN-γ-producing splenocytes and numbers of IFN-γ-producing splenocytes (**F**) were calculated from the ELISPOT assay after 20 μg/mL gE stimulation. N = 6, each dot represents an independent mouse. PBS controls were splenocytes from PBS immunized mice stimulated with gE and positive controls were cells stimulated with 12-myristate 13-acetate (PMA) + ionomycin. Data were compared using one-way analysis of variance (ANOVA) followed by Tukey's multiple comparisons test, comparing the mean of each group with the mean of every other group. *, $P < 0.05$; **, $P < 0.01$; ***, $P < 0.001$; ****, $P < 0.0001$.

value of 0.2705% for Shingrix™ and mean value of 0.2498% for the LNP vaccine, $P = 0.9942$) or not (mean value of 0.0975% for Shingrix™ and mean value of 0.1460% for the LNP vaccine, $P = 0.7211$) (Fig. 4C). Though primed mice showed higher proportion of Th1 cytokine-expression $CD4^+$ T cells than unprimed mice for both Shingrix™ and the LNP vaccines, significant difference was only detected for the analysis of IFN-γ secreting cells (Fig. 4C) instead of IL-2-expressing cells (Fig. 4B).

### 3.5. *LNP encapsulated gE and CpG ODN induced $CD4^+$ memory T cells at levels comparable to that boosted with Shingrix™*

In addition to the magnitude and type of adaptive immune responses induced, the duration of the immune response should be evaluated for vaccines. According to the flow cytometry analysis (Fig. 5A), the proportion of $CD4^+$ effector memory T cells ($CD44^+CD62L^-$, Fig. 5B) was comparable between Shingrix™ and LNP vaccine-immunized mice when they were primed ($P = 0.3685$) or not ($P = 0.1688$). The proportion of $CD4^+$ central memory T cells ($CD44^+CD62L^+$, Fig. 5C) was also comparable between Shingrix™ and LNP vaccine-immunized mice when they were primed ($P = 0.076$) or not ($P = 0.9389$). To be noticed, none of these groups showed significant differences when compared to corresponding control groups. The primed LNP group showed the highest levels of $CD4^+$ central memory T cells than the control group among all of the groups tested, but still the difference is not significant ($P = 0.0568$).

## 4. Discussion

Silent reactivation of latent VZV from either natural infection or Oka strain vaccination could boost immunity endogenously, likely contributing to the relatively stable antibody levels against VZV in older individuals (Gershon et al., 2015; Hope-Simpson, 1965). This is one rational explanation for the extremely high efficacy of the Oka strain-based varicella vaccine that depends on humoral immunity to prevent VZV infection. From this point of view, the VZV-primed animal model for zoster vaccine evaluation is far from perfect because VZV naturally infects only humans and does not efficiently replicate in experimental animals, including mice and nonhuman primates (Mahalingam et al., 2010; Wroblewska et al., 1993). Despite the absence of skin pathology, which may be partly attributed to the special skin structure of humans compared with that of existing experimental animals, the absence of silent reactivation of latent VZV resulted in only a low humoral response in VZV-primed mice (prime control in Fig. 2B). This finding was consistent with previous reports, where mice were primed once with 10,000 PFU of VZV (one human dose of the varicella vaccine

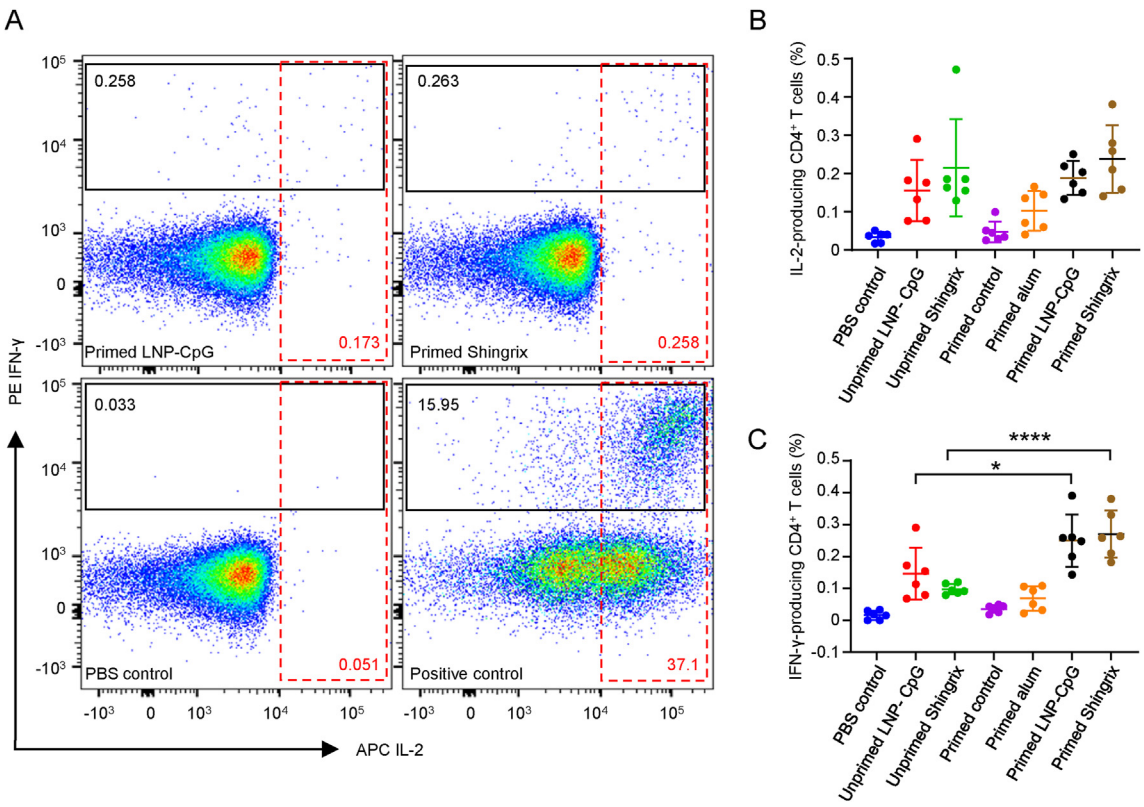


**Fig. 4.** LNP vaccines induced T helper 1 (Th1) cytokine-expressing $CD4^+$ T cells at levels comparable to Shingrix™ in immunized mice as detected by flow cytometry assay. **A** Pseudocolor images displaying representative results near the average value for gated IL-2/IFN-γ-expressing $CD4^+$ T cells. **B** Proportion of IL-2-producing $CD4^+$ T cells among splenocytes after 10 μg/mL gE stimulation. **C** Proportion of IFN-γ-producing $CD4^+$ T cells among splenocytes after 10 μg/mL gE stimulation. N = 6, points represent individual mice. PBS controls were splenocytes from PBS immunized mice stimulated with gE and positive controls were these cells stimulated with $PMA^+$ ionomycin. Data were compared using one-way analysis of variance (ANOVA) followed by Tukey's multiple comparisons test, comparing the mean of each group with the mean of every other group. *, $P < 0.05$; ****, $P < 0.0001$.

Varilrix™) (Dendouga et al., 2012) and rhesus macaques were primed once with ≥ 19,400 PFU of VZV (one human dose of the zoster vaccine ZOSTVAX®) (Monslow et al., 2020). Unlike humoral immunity, the number of functional VZV-specific T cells that control or eliminate reactivated VZV decreases in aged individuals (Arvin, 2005; Levin et al., 2008). From this point of view, the VZV-primed animal model we adopted in this study that was the same as previously used for zoster vaccine evaluation (Dendouga et al., 2012) seems to be suitable because only a low CMI response was detected in VZV-primed mice (Fig. 4B and C), same as previously reported in both mice (Dendouga et al., 2012) and nonhuman primates (Monslow et al., 2020). But still, these seemingly similar CMI responses are different in humans and animals, which make vaccine studies in these animal models can only provide immunogenicity data as indirect clues of vaccine efficacy in humans.

For the humoral response, the priming strategy did not show any benefits in elevating the levels of gE-specific IgG antibodies (Fig. 2B). In fact, unprimed mice showed slightly higher levels of gE-specific IgG antibodies. One explanation for this is that when the priming is considered vaccine immunization, the 0-1-2-month three-dose immunization schedule is not good for higher humoral immunity induction and is even inferior to the 0-1-month two-dose immunization schedule. This phenomenon was confirmed in our unpublished pilot studies. For cytokine responses, the priming strategy increased all of the indexes tested to different levels (Fig. 3). Except for the IL-2 levels in the supernatant of splenocytes from primed mice (mean level of 1143 pg/mL for Shingrix™ and mean level of 779 pg/mL for the LNP vaccine, $P = 0.0235$), the levels of all of the indexes tested in mice immunized with the LNP vaccine were comparable to those in Shingrix™-immunized mice. The absolute value of the IL-2 level was lower than the IFN-γ level in each group of mice, which may have amplified the statistical deviation, especially when the higher outlier values were included (Fig. 3A). Despite the above analysis, clinical trials in humans showed greater association of IL-2 with Shingrix™ than preclinical animal experiments (Cunningham et al., 2018; Monslow et al., 2020). A third boost will be evaluated to elevate this index in our future studies. Besides, the use of Shingrix™ as the positive control has potential limitations in immunogenicity evaluation of this study. While Shingrix™ is produced under GMP conditions, our LNP vaccines were prepared in lab. Ambiguous factors affecting the quality and immunological performance of experimental vaccines, e.g., endotoxin contamination that may make immunogenicity of this LNP vaccine appear strong, are still to be ruled out. In addition, physiochemical characteristics, including size, have been proven to have an important impact on particle vaccine uptake and presentation of loaded immunogens, which could enhance vaccine Th1-type CMI responses (Brewer et al., 1998, 2004; Carstens et al., 2011; He et al., 2021; Henriksen-Lacey et al., 2011; Wui et al., 2019). These characteristics will also be evaluated in our future studies.

gE-specific Th1 $CD4^+$ T cells have been adopted more frequently than $CD8^+$ T cells as good indicators of the potential of zoster vaccines in animal experiments and clinical trials (Cunningham et al., 2018; Dendouga et al., 2012; Laing et al., 2015; Monslow et al., 2020). In this context, when cytokine-producing gE-specific Th1 $CD4^+$ T cells were tested, mice immunized with the LNP vaccine showed comparable levels of all indexes as Shingrix™-immunized mice, all significantly higher than the negative control group, regardless of whether they were primed or not (Fig. 4). Though Shingrix™ showed better results than the LNP vaccines to induce

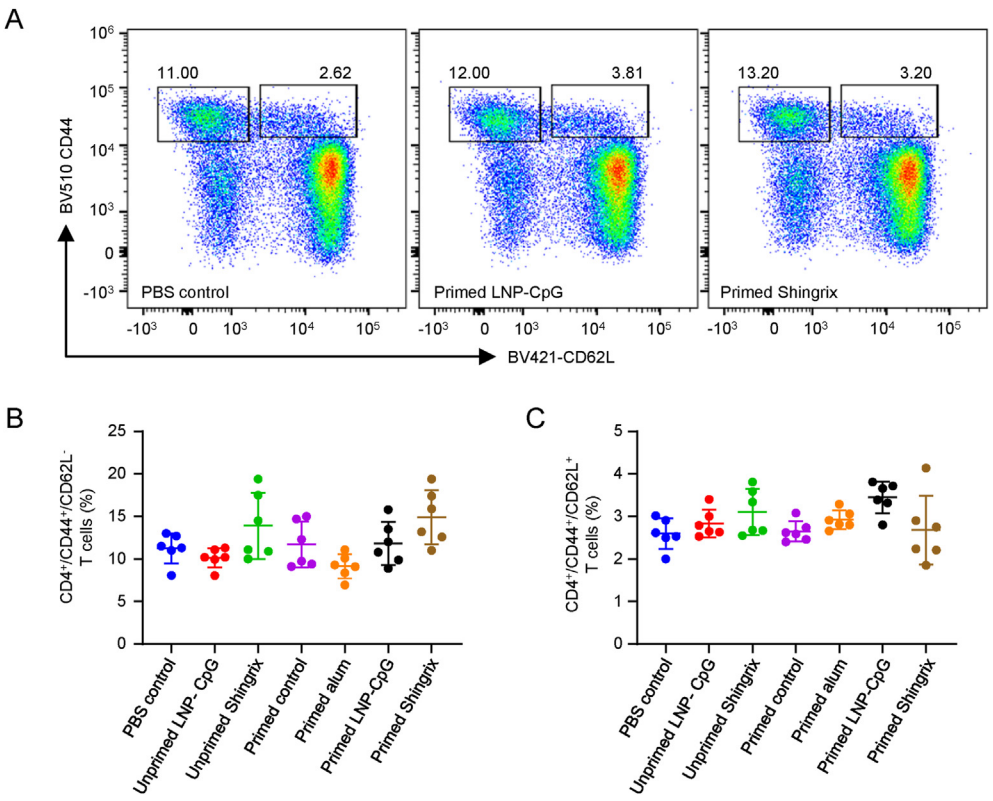


**Fig. 5.** LNP vaccines induced CD4$^+$ memory T cells at levels comparable to Shingrix™ in immunized mice as detected by flow cytometry assay. **A** Pseudocolor images displaying representative results near the average value for gated CD44$^+$/CD62L$^+$ cells. **B** Proportion of effector memory T cells. **C** Proportion of central memory T cells. N = 6, points represent individual mice. Data were compared using one-way analysis of variance (ANOVA) followed by Tukey's multiple comparisons test, comparing the mean of each group with the mean of every other group.

CD4$^+$ effector memory T cells (CD44$^+$CD62L$^-$) (Fig. 5B), the difference between the LNP group and the control group is not significant ($P$ = 0.3307 for the primed groups and $P$ = 0.5607 for the unprimed groups). Similar situation exists for CD4$^+$ central memory T cells (CD44$^+$CD62L$^+$) (Fig. 5C). The primed LNP group showed the highest levels of CD4$^+$ central memory T cells than the control group among all of the groups tested, but still the difference is not significant ($P$ = 0.0568). Previous clinical reports showed that gE-specific CD4$^+$ T cells in healthy people showed a phenotype more compatible with effector memory status, which may explain the recurrence of zoster observed in specific populations and maybe also a great challenge for the long-term protection for zoster vaccines (Malavige et al., 2008). Long-term protection of these LNPs as potential zoster vaccines is still to be proved in clinical trials.

## 5. Conclusions

In conclusion, LNP-CpG-adjuvanted VZV gE, as a subunit zoster vaccine, induced comparable CMI responses to Shingrix™ in the VZV-primed mouse model that was adopted for the evaluation of Shingrix™ in preclinical studies, which showed promise as an effective zoster vaccine. All the components in this LNP vaccine, including the LNP carriers and the CpG ODN stimulators, have been approved by the FDA for use in human vaccines and have shown good safety. All of these components can be artificially and economically synthesized in large quantities, exhibiting potential for the production of more cost-effective zoster vaccines.

## Data availability

All the data from the study are available from the corresponding author upon reasonable request.

## Ethics statement

All animal experiments were approved by the Ethics Committee of Animal Care and Welfare of IMB, CAMS, and by the Yunnan Provincial Experimental Animal Management Association (permit number: SYXK (dian) K2019-0003).

## Author contributions

Ning Luan: investigation, formal analysis, writing-original draft. Han Cao: methodology, data curation. Yunfei Wang: investigation. Kangyang Lin: investigation. Cunbao Liu: Conceptualization, funding acquisition, supervision, writing-original draft, writing-review & editing.

## Conflict of interest

The authors declare that they have no conflicts of interest.

## Acknowledgments

This work was supported by the Major Science and Technology Special Projects of Yunnan Province, China (202002AA100009), the Non-profit Central Research Institute Fund of Chinese Academy of Medical Sciences (2021-JKCS-012), the Special Biomedicine Projects of Yunnan Province (202102AA310035), National Natural Science Foundation of China (82104130), Fundamental Research Funds for the Central Universities (3332021072), the Basic Research Projects of Yunnan Province (202101AU070176, 202101AT070286), the Funds for the Training of High-level Health Technical Personnel in Yunnan Province (grant number H-2019063) and the Funds for High-level Scientific and

Technological Talents Selection Special Project of Yunnan Province (202205AC160015).

## References


Arruti, M., Pineiro, L.D., Salicio, Y., Cilla, G., Goenaga, M.A., Lopez de Munain, A., 2017. Incidence of varicella zoster virus infections of the central nervous system in the elderly: a large tertiary hospital-based series (2007-2014). J. Neurovirol. 23, 451–459.

Arvin, A., 2005. Aging, immunity, and the varicella-zoster virus. N. Engl. J. Med. 352, 2266–2267.

Asada, H., 2019. VZV-specific cell-mediated immunity, but not humoral immunity, correlates inversely with the incidence of herpes zoster and the severity of skin symptoms and zoster-associated pain: the SHEZ study. Vaccine 37, 6776–6781.

Baxter, R., Ray, P., Tran, T.N., Black, S., Shinefield, H.R., Coplan, P.M., Lewis, E., Fireman, B., Saddier, P., 2013. Long-term effectiveness of varicella vaccine: a 14-Year, prospective cohort study. Pediatrics 131, e1389–1396.

Berarducci, B., Ikoma, M., Stamatis, S., Sommer, M., Grose, C., Arvin, A.M., 2006. Essential functions of the unique N-terminal region of the varicella-zoster virus glycoprotein E ectodomain in viral replication and in the pathogenesis of skin infection. J. Virol. 80, 9481–9496.

Breuer, J., 2018. Molecular genetic insights into varicella zoster virus (VZV), the vOka vaccine strain, and the pathogenesis of latency and reactivation. J. Infect. Dis. 218, S75–S80.

Brewer, J.M., Pollock, K.G., Tetley, L., Russell, D.G., 2004. Vesicle size influences the trafficking, processing, and presentation of antigens in lipid vesicles. J. Immunol. 173, 6143–6150.

Brewer, J.M., Tetley, L., Richmond, J., Liew, F.Y., Alexander, J., 1998. Lipid vesicle size determines the Th1 or Th2 response to entrapped antigen. J. Immunol. 161, 4000–4007.

Cao, H., Wang, Y., Luan, N., Liu, C., 2021a. Immunogenicity of varicella-zoster virus glycoprotein E formulated with lipid nanoparticles and. Nucleic Immunostimulators in Mice. Vaccines (Basel) 9, 310.

Cao, H., Yang, S., Wang, Y., Luan, N., Yin, X., Lin, K., Liu, C., 2021b. An established Th2-oriented response to an alum-adjuvanted SARS-CoV-2 subunit vaccine is not reversible by sequential immunization with nucleic acid-adjuvanted Th1-oriented subunit vaccines. Vaccines 9, 1261.

Carstens, M.G., Camps, M.G., Henriksen-Lacey, M., Franken, K., Ottenhoff, T.H., Perrie, Y., Bouwstra, J.A., Ossendorp, F., Jiskoot, W., 2011. Effect of vesicle size on tissue localization and immunogenicity of liposomal DNA vaccines. Vaccine 29, 4761–4770.

Chlibek, R., Bayas, J.M., Collins, H., de la Pinta, M.L., Ledent, E., Mols, J.F., Heineman, T.C., 2013. Safety and immunogenicity of an AS01-adjuvanted varicella-zoster virus subunit candidate vaccine against herpes zoster in adults >=50 years of age. J. Infect. Dis. 208, 1953–1961.

Cohen, J.I., 2015. A new vaccine to prevent herpes zoster. N. Engl. J. Med. 372, 2149–2150.

Cunningham, A.L., Heineman, T.C., Lal, H., Godeaux, O., Chlibek, R., Hwang, S.J., McElhaney, J.E., Vesikari, T., Andrews, C., Choi, W.S., Esen, M., Ikematsu, H., Choma, M.K., Pauksens, K., Ravault, S., Salaun, B., Schwarz, T.F., Smetana, J., Abeele, C.V., Van den Steen, P., Vastiau, I., Weckx, L.Y., Levin, M.J., Group, Z.O.E.S., 2018. Immune responses to a recombinant glycoprotein E herpes zoster vaccine in adults aged 50 Years or older. J. Infect. Dis. 217, 1750–1760.

Cunningham, A.L., Lal, H., Kovac, M., Chlibek, R., Hwang, S.J., Diez-Domingo, J., Godeaux, O., Levin, M.J., McElhaney, J.E., Puig-Barbera, J., Vanden Abeele, C., Vesikari, T., Watanabe, D., Zahaf, T., Ahonen, A., Athan, E., Barba-Gomez, J.F., Campora, L., de Looze, F., Downey, H.J., Ghesquiere, W., Gorfinkel, I., Korhonen, T., Leung, E., McNeil, S.A., Oostvogels, L., Rombo, L., Smetana, J., Weckx, L., Yeo, W., Heineman, T.C., Group, Z.O.E.S., 2016. Efficacy of the herpes zoster subunit vaccine in adults 70 Years of age or older. N. Engl. J. Med. 375, 1019–1032.

Dendouga, N., Fochesato, M., Lockman, L., Mossman, S., Giannini, S.L., 2012. Cell-mediated immune responses to a varicella-zoster virus glycoprotein E vaccine using both a TLR agonist and QS21 in mice. Vaccine 30, 3126–3135.

Garcia-Valcarcel, M., Fowler, W.J., Harper, D.R., Jeffries, D.J., Layton, G.T., 1997. Induction of neutralizing antibody and T-cell responses to varicella-zoster virus (VZV) using Ty-virus-like particles carrying fragments of glycoprotein E (gE). Vaccine 15, 709–719.

Gershon, A.A., Breuer, J., Cohen, J.I., Cohrs, R.J., Gershon, M.D., Gilden, D., Grose, C., Hambleton, S., Kennedy, P.G., Oxman, M.N., Seward, J.F., Yamanishi, K., 2015. Varicella zoster virus infection. Nat. Rev. Dis. Prim. 1, 15016.

Gilbert, P.B., Gabriel, E.E., Miao, X., Li, X., Su, S.C., Parrino, J., Chan, I.S., 2014. Fold rise in antibody titers by measured by glycoprotein-based enzyme-linked immunosorbent assay is an excellent correlate of protection for a herpes zoster vaccine, demonstrated via the vaccine efficacy curve. J. Infect. Dis. 210, 1573–1581.

Gilderman, L.I., Lawless, J.F., Nolen, T.M., Sterling, T., Rutledge, R.Z., Fernsler, D.A., Azrolan, N., Sutradhar, S.C., Wang, W.W., Chan, I.S., Schlienger, K., Schodel, F., Silber, J.L., Zostavax Protocol 010 Study, G., 2008. A double-blind, randomized, controlled, multicenter safety and immunogenicity study of a refrigerator-stable formulation of Zostavax. Clin. Vaccine Immunol. 15, 314–319.

Haberthur, K., Engelmann, F., Park, B., Barron, A., Legasse, A., Dewane, J., Fischer, M., Kerns, A., Brown, M., Messaoudi, I., 2011. CD4 T cell immunity is critical for the control of simian varicella virus infection in a nonhuman primate model of VZV infection. PLoS Pathog. 7, e1002367.

Hales, C.M., Harpaz, R., Joesoef, M.R., Bialek, S.R., 2013. Examination of links between herpes zoster incidence and childhood varicella vaccination. Ann. Intern. Med. 159, 739–745.

Haumont, M., Jacquet, A., Massaer, M., Deleersnyder, V., Mazzu, P., Bollen, A., Jacobs, P., 1996. Purification, characterization and immunogenicity of recombinant varicella-zoster virus glycoprotein gE secreted by Chinese hamster ovary cells. Virus Res. 40, 199–204.

He, L., Sun, B., Guo, Y., Yan, K., Liu, D., Zang, Y., Jiang, C., Zhang, Y., Kong, W., 2021. Immune response of C57BL/6J mice to herpes zoster subunit vaccines formulated with nanoemulsion-based and liposome-based adjuvants. Int. Immunopharm. 101, 108216.

Henriksen-Lacey, M., Devitt, A., Perrie, Y., 2011. The vesicle size of DDA:TDB liposomal adjuvants plays a role in the cell-mediated immune response but has no significant effect on antibody production. J. Contr. Release 154, 131–137.

Hope-Simpson, R.E., 1965. The nature of herpes zoster: a long-term study and a new hypothesis. Proc. Roy. Soc. Med. 58, 9–20.

Iqbal, M., Zafar, N., Fessi, H., Elaissari, A., 2015. Double emulsion solvent evaporation techniques used for drug encapsulation. Int. J. Pharm. 496, 173–190.

Johnson, R.W., Rice, A.S., 2014. Clinical practice. Postherpetic neuralgia. N. Engl. J. Med. 371, 1526–1533.

Krause, P.R., Klinman, D.M., 2000. Varicella vaccination: evidence for frequent reactivation of the vaccine strain in healthy children. Nat. Med. 6, 451–454.

Laing, K.J., Russell, R.M., Dong, L., Schmid, D.S., Stern, M., Magaret, A., Haas, J.G., Johnston, C., Wald, A., Koelle, D.M., 2015. Zoster vaccination increases the breadth of CD4+ T cells responsive to varicella zoster virus. J. Infect. Dis. 212, 1022–1031.

Lee, T., Suh, J., Choi, J.K., Lee, J., Park, S.H., 2021. Estimating the basic reproductive number of varicella in South Korea incorporating social contact patterns and seroprevalence. Hum. Vaccines Immunother. 17, 2488–2493.

Leroux-Roels, I., Leroux-Roels, G., Clement, F., Vandepapeliere, P., Vassilev, V., Ledent, E., Heineman, T.C., 2012. A phase 1/2 clinical trial evaluating safety and immunogenicity of a varicella zoster glycoprotein e subunit vaccine candidate in young and older adults. J. Infect. Dis. 206, 1280–1290.

Leung, J., Harpaz, R., Molinari, N.A., Jumaan, A., Zhou, F., 2011. Herpes zoster incidence among insured persons in the United States, 1993-2006: evaluation of impact of varicella vaccination. Clin. Infect. Dis. 52, 332–340.

Levin, M.J., Bresnitz, E., Popmihajlov, Z., Weinberg, A., Liaw, K.L., Willis, E., Curtis, J.R., 2017. Studies with herpes zoster vaccines in immune compromised patients. Expert Rev. Vaccines 16, 1217–1230.

Levin, M.J., Oxman, M.N., Zhang, J.H., Johnson, G.R., Stanley, H., Hayward, A.R., Caulfield, M.J., Irwin, M.R., Smith, J.G., Clair, J., Chan, I.S., Williams, H., Harbecke, R., Marchese, R., Straus, S.E., Gershon, A., Weinberg, A., Veterans Affairs Cooperative Studies Program Shingles Prevention Study, I., 2008. Varicella-zoster virus-specific immune responses in elderly recipients of a herpes zoster vaccine. J. Infect. Dis. 197, 825–835.

Liu, C., Chu, X., Sun, P., Feng, X., Huang, W., Liu, H., Ma, Y., 2018a. Synergy effects of Polyinosinic-polycytidylic acid, CpG oligodeoxynucleotide, and cationic peptides to adjuvant HPV E7 epitope vaccine through preventive and therapeutic immunization in a TC-1 grafted mouse model. Hum. Vaccines Immunother. 14, 931–940.

Liu, C., Chu, X., Yan, M., Qi, J., Liu, H., Gao, F., Gao, R., Ma, G., Ma, Y., 2018b. Encapsulation of Poly I:C and the natural phosphodiester CpG ODN enhanced the efficacy of a hyaluronic acid-modified cationic lipid-PLGA hybrid nanoparticle vaccine in TC-1-grafted tumors. Int. J. Pharm. 553, 327–337.

Liu, C., Huang, P., Zhao, D., Xia, M., Zhong, W., Jiang, X., Tan, M., 2021. Effects of rotavirus NSP4 protein on the immune response and protection of the SR69A-VP8* nanoparticle rotavirus vaccine. Vaccine 39, 263–271.

Mahalingam, R., Messaoudi, I., Gilden, D., 2010. Simian varicella virus pathogenesis. Curr. Top. Microbiol. Immunol. 342, 309–321.

Malavige, G.N., Jones, L., Black, A.P., Ogg, G.S., 2008. Varicella zoster virus glycoprotein E-specific CD4+ T cells show evidence of recent activation and effector differentiation, consistent with frequent exposure to replicative cycle antigens in healthy immune donors. Clin. Exp. Immunol. 152, 522–531.

Mo, C., Lee, J., Sommer, M., Grose, C., Arvin, A.M., 2002. The requirement of varicella zoster virus glycoprotein E (gE) for viral replication and effects of glycoprotein I on gE in melanoma cells. Virology 304, 176–186.

Mo, C., Schneeberger, E.E., Arvin, A.M., 2000. Glycoprotein E of varicella-zoster virus enhances cell-cell contact in polarized epithelial cells. J. Virol. 74, 11377–11387.

Moffat, J., Mo, C., Cheng, J.J., Sommer, M., Zerboni, L., Stamatis, S., Arvin, A.M., 2004. Functions of the C-terminal domain of varicella-zoster virus glycoprotein E in viral replication in vitro and skin and T-cell tropism in vivo. J. Virol. 78, 12406–12415.

Monslow, M.A., Elbashir, S., Sullivan, N.L., Thiriot, D.S., Ahl, P., Smith, J., Miller, E., Cook, J., Cosmi, S., Thoryk, E., Citron, M., Thambi, N., Shaw, C., Hazuda, D., Vora, K.A., 2020. Immunogenicity generated by mRNA vaccine encoding VZV gE antigen is comparable to adjuvanted subunit vaccine and better than live attenuated vaccine in nonhuman primates. Vaccine 38, 5793–5802.

Ogunjimi, B., Hens, N., Goeyvaerts, N., Aerts, M., Van Damme, P., Beutels, P., 2009. Using empirical social contact data to model person to person infectious disease transmission: an illustration for varicella. Math. Biosci. 218, 80–87.

Oxman, M.N., Levin, M.J., Johnson, G.R., Schmader, K.E., Straus, S.E., Gelb, L.D., Arbeit, R.D., Simberkoff, M.S., Gershon, A.A., Davis, L.E., Weinberg, A., Boardman, K.D., Williams, H.M., Zhang, J.H., Peduzzi, P.N., Beisel, C.E., Morrison, V.A., Guatelli, J.C., Brooks, P.A., Kauffman, C.A., Pachucki, C.T., Neuzil, K.M., Betts, R.F., Wright, P.F., Griffin, M.R., Brunell, P., Soto, N.E., Marques, A.R., Keay, S.K., Goodman, R.P., Cotton, D.J., Gnann Jr., J.W., Loutit, J., Holodniy, M., Keitel, W.A., Crawford, G.E., Yeh, S.S., Lobo, Z., Toney, J.F., Greenberg, R.N., Keller, P.M., Harbecke, R., Hayward, A.R., Irwin, M.R., Kyriakides, T.C., Chan, C.Y., Chan, I.S., Wang, W.W., Annunziato, P.W., Silber, J.L., Shingles Prevention Study, G., 2005. A vaccine to prevent herpes zoster and postherpetic neuralgia in older adults. N. Engl. J. Med. 352, 2271–2284.

Steain, M., Sutherland, J.P., Rodriguez, M., Cunningham, A.L., Slobedman, B., Abendroth, A., 2014. Analysis of T cell responses during active varicella-zoster virus reactivation in human ganglia. J. Virol. 88, 2704–2716.
Takahashi, M., Otsuka, T., Okuno, Y., Asano, Y., Yazaki, T., 1974. Live vaccine used to prevent the spread of varicella in children in hospital. Lancet 2, 1288–1290.
Upadhyay, S., Jeena, G.S., Shikha, Shukla, R.K., 2018. Recent advances in steroidal saponins biosynthesis and in vitro production. Planta 248, 519–544.
Wang, P., 2021. Natural and synthetic saponins as vaccine adjuvants. Vaccines 9, 222.
Wang, Y., Qi, J., Cao, H., Liu, C., 2021. Immune responses to varicella-zoster virus glycoprotein E formulated with poly(lactic-co-glycolic acid) nanoparticles and nucleic acid adjuvants in mice. Virol. Sin. 36, 122–132.
Weinberg, A., Levin, M.J., 2010. VZV T cell-mediated immunity. Curr. Top. Microbiol. Immunol. 342, 341–357.
Wroblewska, Z., Valyi-Nagy, T., Otte, J., Dillner, A., Jackson, A., Sole, D.P., Fraser, N.W., 1993. A mouse model for varicella-zoster virus latency. Microb. Pathog. 15, 141–151.
Wui, S.R., Kim, K.S., Ryu, J.I., Ko, A., Do, H.T.T., Lee, Y.J., Kim, H.J., Lim, S.J., Park, S.A., Cho, Y.J., Kim, C.G., Lee, N.G., 2019. Efficient induction of cell-mediated immunity to varicella-zoster virus glycoprotein E co-lyophilized with a cationic liposome-based adjuvant in mice. Vaccine 37, 2131–2141.
Zhu, R., Liu, J., Chen, C., Ye, X., Xu, L., Wang, W., Zhao, Q., Zhu, H., Cheng, T., Xia, N., 2016. A highly conserved epitope-vaccine candidate against varicella-zoster virus induces neutralizing antibodies in mice. Vaccine 34, 1589–1596.